

Published in final edited form as:

Oncogene. 2015 July 30; 34(31): 4118–4129. doi:10.1038/onc.2014.342.

Apc and p53 interaction in DNA damage and genomic instability in hepatocytes

Valérie Méniel^{§,1}, Matthias Megges², Madeleine A Young¹, Alicia Cole³, Owen J Sansom³, and Alan R Clarke¹

¹European Cancer Stem Cell Research Institute, Cardiff University, CF24 4HQ Cardiff, UK

²Max Planck Institute for Molecular Genetics, Ihnestraße 63-73, 14195 Berlin, Germany

³The Beatson institute for Cancer Research, Switchback Road, Glasgow G61 1BD, UK

Abstract

Disruption of Apc within hepatocytes activates Wnt signaling, perturb differentiation and ultimately lead to neoplasia. Apc negatively regulates Wnt signaling but is also involved in organizing the cytoskeleton and may play a role in chromosome segregation. *In vitro* studies have implicated Apc in the control of genomic stability. However, the relevance of this data has been questioned *in vivo* as Apc is lost earlier than the onset of genomic instability. Here, we analyse the relationship between immediate loss of Apc and the acquisition of genomic instability in hepatocytes. We used Cre-lox technology to inactivate Apc and in combination with p53 *in vivo*, to define the consequences of gene loss upon cell-cycle regulation, proliferation, death and aneuploidy. We show that whilst Apc loss leads to increased proliferation, it also leads to increased apoptosis, the accumulation of p53, p21 and markers of DSBs and DNA repair. Flow cytometry revealed an increased 4N DNA content, consistent with a G2 arrest. Levels of anaphase bridges were also elevated, implicating failed chromosome segregation. This was accompanied by an increase in centrosome number which demonstrates a role for Apc in maintaining euploidy.

To address the role of p53 in these processes, we analyzed combined loss of Apc and p53, which led to a further increase in proliferation, cell death, DNA damages and repair and a bypass of G2 arrest than was observed with Apc loss. However we observed only a marginal effect on anaphase bridges and centrosome number which could be due to increased cell death. Our data therefore establishes, in an *in vivo* setting, that APC loss leads to a DNA damage signature and genomic instability in the liver and that additional loss of p53 leads to an increase in the DNA damage signal but not to an immediate increase in the genomic instability phenotype.

Users may view, print, copy, and download text and data-mine the content in such documents, for the purposes of academic research, subject always to the full Conditions of use:http://www.nature.com/authors/editorial_policies/license.html#terms

[§]Corresponding author: Valérie Méniel: European Cancer Stem Cell Research Institute, Cardiff University, CF24 4HQ, Cardiff, UK; Menielvs@cf.ac.uk; Fax number: 00442920874116 .

The authors declare no conflict of interest

Introduction

Inactivation of the *APC* (adenomatous polyposis coli) gene marks one of the earliest events in colorectal cancer (CRC) [1]. *Apc* is part of the destruction complex that controls the level of β -catenin in the Wnt signaling pathway [2]. However, *Apc* is also involved in the organization of the cytoskeleton, the regulation of cell migration and localizes to kinetochores, centrosomes and microtubules [3-7]. Indeed, APC may regulate kinetochore-microtubule attachment at centrosomes and this could influence centrosome duplication or nucleation during mitosis. Mouse embryonic stem cells (ES) homozygous for *Apc*^{Min} (*Apc*⁸⁵⁰) display extensive chromosome and spindle aberrations, providing genetic evidence for a role of APC in chromosome segregation [3]. All this is suggestive that *Apc* may be important in maintaining genomic stability (GI), and therefore that *Apc* loss may also drive CRC through the acquisition of GI. To this end it has been suggested that GI is an early hallmark of CRC [3,4,8]. However, there remains some controversy over the stage at which GI is acquired, as adenomas driven by *Apc* gene deletion are thought to be genetically stable.

Previously we have shown that *Apc* loss in MEFs and the murine intestinal epithelium leads to an increase in DNA damage, nuclear atypia, upregulation of p53 and p21 and an increase in cells with DNA greater than 4N, suggesting tetraploidy [5]. However, p53 only weakly altered the immediate phenotype of *Apc* loss in the mouse intestine [9]. In the kidney, it was previously found that *Apc* deficiency results in a predisposition to renal carcinoma and that p53 deficiency accelerated the onset of tumour formation [10].

Within adenomas formed after β -catenin activation or *Apc*⁷¹⁶ truncation, an increase in anaphase bridges has been reported, therefore suggesting a level of chromosome instability (CIN) [11]. Consistent with this, a high index of anaphase bridges was found in gastric cancers with Wnt signaling activation and it was suggested that p53 dysfunction and Wnt signaling may cooperate to increase CIN in the progression of the intestinal-type gastric cancer [11].

Wnt signaling is a major pathway involved in the control of liver metabolism and zonation [12]. Activation of Wnt signaling is also a key oncogenic event in hepatocellular carcinoma (HCC) [13]. Several Wnt pathway components have been implicated in HCC such as *Axin2* and *APC* [14-16]. For example, conditional deletion of *Axin1* has been shown to lead to HCC in mice [15] and hypermethylation of the sense strand of the *APC* gene has been shown to be specific for hepatocellular carcinoma [16]. P53 has also been shown to be mutated in HCC [17] and has been shown to have a role in CIN in human HCC [14, 18], but is mutated only late in disease progression.

Given this strong association of deregulated Wnt signaling and HCC, we have used Cre-lox technology to delete *Apc* within mouse hepatocytes. Following Cre induction, mice developed hepatomegaly, with an increase in hepatocyte proliferation [19]. The phenotype was shown to be due to a deregulation of the Wnt pathway as co-deletion of β -catenin following *Apc* loss rescued these phenotypes [19]. Using this clean genetic system (lacking other events that occur during carcinogenesis) we tested whether *Apc* loss directly leads to

GI. Given the cooperation of Apc and p53 loss in driving liver carcinogenesis, we also assessed whether additional deletion of p53 had a direct role in GI driven by Apc deletion.

Results

Loss of Apc in the liver leads to DNA damage, DNA repair and proliferation

Induction of *AhCre*⁺ mice with β -naphthoflavone delivers high levels of recombination in the liver [19]. To yield near 100% recombination in hepatocytes we induced male mice with 3 injections of β -naphthoflavone, however the *AhCre*⁺*Apc*^{fl/fl} mice became ill due to the previously described intestinal phenotype [24] at D4 and were therefore killed. In order to allow the mouse to progress to a more advanced phenotype in hepatocytes we induced female mice (as they usually have lower recombination rates in the intestine) with a single injection of β -naphthoflavone and sacrificed the mice at D6. This protocol leads to a lower level of recombination in the intestine, but retains high levels of recombination in the liver, as evidenced by elevated nuclear β -catenin as a surrogate marker for Apc recombination (>80%) in *AhCre*⁺*Apc*^{fl/fl} at D4 and D6 (FigSup1A-B).

As previously shown [19], we confirmed that Apc loss leads to hepatomegaly (FigSup1C), and determined that this was not a result of increased cell size (FigSup1D). We next determined if hepatomegaly was reflected by an increase in BrdU incorporation (which labels cells in S phase) or Ki67 levels (which labels cells in active phases of the cell cycle (G(1), S, G(2), and mitosis)). At both time points, both markers of proliferation were elevated (Fig1A-B, SupFig1E-F) in *AhCre*⁺*Apc*^{fl/fl} compared to Wt mice (Ki67: D4 and D6 P<0.05 MW; BrdU: D4 P<0.05 MW; D6 P>0.05 MW).

Given Apc loss was causing inappropriate proliferation of differentiated hepatocytes and the data linking Apc and GI, we next investigated whether loss of Apc was inducing the DNA damage checkpoint proteins p53 and p21. Following Apc loss, we found hepatocytes with significantly upregulated expression of p53 (D4: 0.58% Wt vs 11.45% *AhCre*⁺*Apc*^{fl/fl}, P=0.01 MW; D6: 0.09% Wt vs 8.5% *AhCre*⁺*Apc*^{fl/fl} P=0.0152 MW) (Fig1C; FigSup2C) and hepatocytes with elevated p21 (D4:1.6% Wt vs 14.97% *AhCre*⁺*Apc*^{fl/fl} P=0.0404; D6:1.18% Wt vs 9.19% *AhCre*⁺*Apc*^{fl/fl} P=0.0404 MW)(Fig1C; FigSup2D). This suggests the presence of DNA damage due to Apc deficiency. To test if the loss of Apc leads to an increase in double strand breaks (DSB), we carried out IHC analysis of γ H2AX and Rad51 at D4 and D6. At D4 we observed a significant increase in γ -H2AX and Rad51 levels in *AhCre*⁺*Apc*^{fl/fl} (γ -H2AX: D4: 0.9% Wt vs 26.2% *AhCre*⁺*Apc*^{fl/fl} P=0.0404 MW; Rad51: 2% Wt vs 9.9% *AhCre*⁺*Apc*^{fl/fl} P=0.0404 MW) (Fig1E-H). At D6, we observed a significant increase in Rad51 levels in *AhCre*⁺*Apc*^{fl/fl} levels (0.5% Wt vs 50.1% *AhCre*⁺*Apc*^{fl/fl} P=0.0404 MW). There is a similar trend for γ -H2AX but the levels did not reach significance (0.9% Wt vs 4.3% *AhCre*⁺*Apc*^{fl/fl} P=0.0553 MW) (Fig1E-H). These data clearly indicate that loss of Apc leads to the production of DSBs and subsequently DNA repair with the consequent upregulation of p53 and p21.

Apc deficiency leads to increased apoptosis, nuclear area, 4N DNA content and cell cycle perturbation

To determine if the DSBs formation is related to an increase in apoptosis, we scored the number of apoptotic cells stained with active-Caspase3 antibody (Fig1D). At D6 we observed higher numbers of Caspase3 positive cells in *AhCre⁺Apc^{fl/fl}* (0.62%) compared to Wt (0.09%) (MW P=0.0404). A similar trend was observed at D4 but this did not reach significance.

Previously, we have shown that Apc loss increases nuclear area of a subset of intestinal crypt cells implicating possible polyploidy [5]. We therefore analysed if similar changes were occurring in hepatocytes after loss of Apc by measuring nuclear area. Cytological analysis showed enlarged nuclei in *AhCre⁺Apc^{fl/fl}* compared to Wt at D4 and D6 (Fig2A-B). Cumulative plots of the nuclear area (Figure2C-D) showed *AhCre⁺Apc^{fl/fl}* mice have increased nuclear area at both time points compared to the Wt (P=0.01, Kolmogorov–Smirnov).

The increase in nuclear area is suggestive of increased aneuploidy or polyploidy following loss of Apc. To further explore this we next analysed the DNA content of hepatocytes by Flow cytometry. At D4 (Fig2E), we observed a decrease in the number of cells with 2N DNA content in *AhCre⁺Apc^{fl/fl}* (33.22%) compared to Wt (58.83%) (P=0.0404 MW) and an increase in the number of cells with 4N DNA content (*AhCre⁺Apc^{fl/fl}* 48% vs Wt 31.07%, P=0.0404, MW). The same trend was observed at D6 (Fig2F) (2N: Wt 54.17% vs *AhCre⁺Apc^{fl/fl}* 40.1%, P=0.0778 MW; 4N: *AhCre⁺Apc^{fl/fl}* 44.17% vs Wt 36.37%, P=0.0778, MW). We observed no significant difference in cells in S phase between Wt and *AhCre⁺Apc^{fl/fl}* at both time point (SupFig3) which is in contrary to what was observed with the proliferation markers BrdU and Ki67. This could be due to the inability of FACS analysis to detect with high sensitivity the very small percentage of cells in S phase.

One possible interpretation of the decrease in cells with 2N DNA content and the accumulation of cells at 4N is that cells may be arrested in G2 phase after Apc loss. A second possibility is that the elevated 4N population reflects polyploidy. To test the hypothesis that loss of Apc causes G2 arrest we analyzed the fate of cells after a pulse of BrdU labelling. BrdU labels the DNA of cells entering S phase. We hypothesised that any cells that arrested in G2 would reduce the number of BrdU labelled daughter cells generated. Mice were induced with β -naphthoflavone, injected with BrdU and dissected 2hrs or 24hrs after BrdU labelling (Fig1B). At D4, 2hrs after BrdU labelling, the number of BrdU positive cells is greater in *AhCre⁺Apc^{fl/fl}* (1.77%) compared to Wt (0.28%) (MW P=0.0404). However the number of BrdU positive cells remains the same in *AhCre⁺Apc^{fl/fl}* from 2hrs to 24hrs (% positive cells 2hrs: 1.77% vs 24hrs:1.98%, P=0.4298, MW). This suggests that the cells dividing at 2hrs do not give rise to new dividing cells and implies either cell cycle arrest or loss of daughter cells through increased cell death. Similar data were seen at D6 (Fig1B). In contrast, although only few cells were cycling in the Wt livers, rates of BrdU incorporation rose from 2hrs to 24hrs (D4-2hrs: 0.28% vs D4-24hrs 0.50%, P=0.1884 MW; D6-2hrs: 0.45% vs D6-24hrs 0.76%, P=0.1884 MW).

To further test our hypothesis that loss of Apc causes G2 arrest, we performed dual immunostaining with Phospho-Histone H3 (P-histone H3) and BrdU 24hrs after injection of BrdU. P-histone H3 expression serves as a good marker for detecting progression into mitosis from late G2, as its expression is detected from late G2 to early telophase [25]. We compared this pattern of staining to BrdU labelling 24hrs after BrdU exposure. We hypothesized that, in the absence of a G2 arrest, cells labelled with BrdU at S phase will proceed to mitosis and label with both BrdU and P-histone H3. In contrast, where there is an arrest, this would be reflected in reduced double labelling of cells. At D4 in Wt mice, the majority of hepatocytes are labelled with both BrdU and P-histone H3 (Fig2I), whereas in *AhCre⁺Apc^{fl/fl}* mice this was considerably reduced (D4: Wt 87% vs *AhCre⁺Apc^{fl/fl}* 23.7%, $P=0.0259$ MW). Similar data were seen at D6 (Wt 66.8% vs *AhCre⁺Apc^{fl/fl}* 28.68%, $P=0.0259$). These data strongly support our hypothesis that loss of Apc leads to a G2 arrest.

Notably, the number of binucleate cells is reduced in *AhCre⁺Apc^{fl/fl}* compared to Wt (SupFig1G; $P=0.0404$, MW). This reduction is P53 dependent as the number of binucleate cells was increased to the Wt level in *AhCre⁺Apc^{fl/fl}P53^{-/-}* mice compared to *AhCre⁺Apc^{fl/fl}* (SupFig1G; $P<0.05$, MW at D6 and D4).

Loss of Apc leads to an increase in anaphase bridges

Previously, the presence of anaphase bridges has been linked to CIN. To determine if Apc loss induces an increase in aberrant mitosis, we scored the anaphase bridge (Fig2H) index in the livers of Wt and *AhCre⁺Apc^{fl/fl}* (Fig2G). We observed at D4 a significantly elevated index after Apc loss (Wt 0% vs *AhCre⁺Apc^{fl/fl}* 10.1%: $p=0.05$). Because all Wt values were zero we used a bootstrapping method to perform the statistical analysis (see Material and methods for detail). We observed the same trend at D6 but the level didn't reach significance.

P53 deficiency enhances the DNA damage signal and cell cycle perturbations induced by Apc loss

Given the upregulation of p53 and p21 after the loss of Apc, we hypothesized that deficiency of p53 may accentuate the abnormalities observed after Apc loss in the liver. We therefore generated *AhCre⁺p53^{-/-}* and *AhCre⁺Apc^{fl/fl}p53^{-/-}* mice. First, we determined if the level of Apc gene deletion was affected by p53 deficiency. At both time points we observed the same levels of recombination (as assessed by nuclear β -catenin) in *AhCre⁺Apc^{fl/fl}p53^{-/-}* mice compared to *AhCre⁺Apc^{fl/fl}* ($P=0.1352$ MW, FigSup1A-B). Next, we measured liver weight and found no effect of additional p53 loss (SupFig1C: *AhCre⁺Apc^{fl/fl}* 2.2gr/mouse vs *AhCre⁺Apc^{fl/fl}p53^{-/-}* 2.16gr/mouse, $P=0.6625$ MW). Histology of the livers of *AhCre⁺p53^{-/-}* and *AhCre⁺Apc^{fl/fl}p53^{-/-}* mice are shown in FigSup2E and compared to Wt and *AhCre⁺Apc^{fl/fl}*. H and E sections do not reveal any morphological differences between *AhCre⁺Apc^{fl/fl}* and *AhCre⁺Apc^{fl/fl}p53^{-/-}* livers.

Given the role of p53 in controlling the level of p21, we next analyzed by IHC the expression levels of p21 (Fig3A+SupFig2D). Levels of P21 staining were low in the *AhCre⁺p53^{-/-}* mice and were elevated and comparable in the *AhCre⁺Apc^{fl/fl}* and *AhCre⁺Apc^{fl/fl}p53^{-/-}* mice, suggesting the increase in p21 is independent of the p53

pathway. We next determined if p53 deficiency would enhance the DNA damage signal following Apc loss at D4. The level of γ -H2AX and Rad51 staining was low in *AhCre⁺p53^{-/-}* mice (γ H2AX: 6.3% (D4), 2.07% (D6); Rad51: 6.8% (D4), 2.7% (D6)) (Fig3B-E). As stated above, deficiency of Apc increased both these levels (γ H2AX: 26.2% (D4), 4.34% (D6); Rad51: 9.9% (D4), 50.1% (D6)). The additional deficiency of p53 in *AhCre⁺Apc^{fl/fl}* further raised levels of both markers (γ H2AX: 67.1% (D4), 10.45% (D6), Rad51: 20.7% (D4), 17.7% (D6) (Fig3B-E). These data indicate an increase in DNA damage in *AhCre⁺Apc^{fl/fl}p53^{-/-}* compared to *AhCre⁺Apc^{fl/fl}* suggesting p53 is a key factor in controlling the level of these DSBs generated after Apc deficiency.

Proliferation in *AhCre⁺Apc^{fl/fl}* mice as scored by Ki67 levels was further significantly increased after additional loss of p53 at D6 (Wt 3.59%; *AhCre⁺p53^{-/-}* 4.09%; *AhCre⁺Apc^{fl/fl}* 19.66%; *AhCre⁺Apc^{fl/fl}p53^{-/-}* 43.29%) and with a similar trend at D4 (Wt 3.81%; *AhCre⁺p53^{-/-}* 7.12%; *AhCre⁺Apc^{fl/fl}* 15.76%; *AhCre⁺Apc^{fl/fl}p53^{-/-}* 29.38%) (Fig3F). Similar results were observed with BrdU analysis (see below).

We next determined the effect of p53 deficiency upon apoptosis as scored by the number of Caspase3 positive cells. At D4 we observed a significant elevation in *AhCre⁺Apc^{fl/fl}p53^{-/-}* vs *AhCre⁺Apc^{fl/fl}* (Wt 0.36%; *AhCre⁺p53^{-/-}* 0.51%; *AhCre⁺Apc^{fl/fl}* 0.66%; *AhCre⁺Apc^{fl/fl}p53^{-/-}* 1.34%). At D6 we observed a similar trend, although the difference did not reach significance in *AhCre⁺Apc^{fl/fl}p53^{-/-}* (Wt 0.09%; *AhCre⁺p53^{-/-}* 0.0%; *AhCre⁺Apc^{fl/fl}* 0.62%; *AhCre⁺Apc^{fl/fl}p53^{-/-}* 0.97%) (Fig3G).

Loss of Apc leads to an increase in nuclear area in the liver hepatocytes compared to Wt and compared to *AhCre⁺p53^{-/-}* (P=0.01, Kolmogorov-Smirnov, Fig2A-D and Fig4A-D). However additional loss of p53 enhanced the Apc phenotype (P=0.01, Kolmogorov-Smirnov, Fig2A-D and Fig4A-D). Of interest, P53 deficiency alone did alter nuclear area compared to Wt (P=0.01, Kolmogorov-Smirnov) (SupFig2A-B).

We next analysed the DNA content of hepatocytes in *AhCre⁺Apc^{fl/fl}p53^{-/-}*. At D4 *AhCre⁺Apc^{fl/fl}p53^{-/-}* showed an increase in 2N DNA content to approximately Wt levels (Wt 58.83%; *AhCre⁺p53^{-/-}* 52.89%; *AhCre⁺Apc^{fl/fl}* 33.22%; *AhCre⁺Apc^{fl/fl}p53^{-/-}* 52.54%), and a marked reduction in 4N DNA content (Wt 31.07%; *AhCre⁺p53^{-/-}* 20.79%; *AhCre⁺Apc^{fl/fl}* 48.0%; *AhCre⁺Apc^{fl/fl}p53^{-/-}* 15.49%) (Fig2E-4E). At D6 a similar pattern was observed in both the 2N (Wt 54.17%; *AhCre⁺p53^{-/-}* 47.78%; *AhCre⁺Apc^{fl/fl}* 40.1%; *AhCre⁺Apc^{fl/fl}p53^{-/-}* 44.11%), and 4N DNA content (Wt 36.37%; *AhCre⁺p53^{-/-}* 28.8%; *AhCre⁺Apc^{fl/fl}* 44.17%; *AhCre⁺Apc^{fl/fl}p53^{-/-}* 18.71%) (Fig2F-4F). Both time points analysed are consistent with a loss of G2 checkpoint activity in *AhCre⁺Apc^{fl/fl}p53^{-/-}*.

We also analysed percentage of cells with DNA content greater than 4N. At D4 we found a marked increase in *AhCre⁺Apc^{fl/fl}p53^{-/-}* (Wt 18.47%; *AhCre⁺p53^{-/-}* 14.61%; *AhCre⁺Apc^{fl/fl}* 16.62%; *AhCre⁺Apc^{fl/fl}p53^{-/-}* 24.9%), which was also seen at D6 (Wt 7.66%; *AhCre⁺p53^{-/-}* 20.94%; *AhCre⁺Apc^{fl/fl}* 13.45%; *AhCre⁺Apc^{fl/fl}p53^{-/-}* 31.93%) (Fig2E-F, 4E-F). This data clearly suggests that in a p53 deficient background, Apc deficient cells undergo an increase in ploidy.

To further address the hypothesis that loss of Apc causes a p53 dependent G2 arrest we analysed the fate of cells after a pulse of BrdU labelling. At D4, the number of BrdU positive cells 2hrs after labelling was significantly greater in *AhCre⁺Apc^{fl/fl}p53^{-/-}* (4.48%) compared to *AhCre⁺Apc^{fl/fl}* (1.77%) mice (Fig3H), consistent with our previous observations of elevated Ki67 in *AhCre⁺Apc^{fl/fl}p53^{-/-}*. However, the number of BrdU positive cells (Fig3H) remained the same in *AhCre⁺Apc^{fl/fl}P53^{-/-}* from 2-24hrs (P=0.3313 MW). Similar data was obtained at D6 (Fig3I), suggesting that at both time points there was a balance between proliferation and cell death.

To further address our hypothesis of a bypass of G2 arrest caused by Apc loss and combined P53 deficiency we again performed double labelling with BrdU (24hrs) and P-histone H3 in *AhCre⁺p53^{-/-}* and *AhCre⁺Apc^{fl/fl}p53^{-/-}* mice and compared them to Wt and *AhCre⁺Apc^{fl/fl}* controls. At both D4 and D6 we observed (Fig5A-C) an increase in the number of cells labelled with both BrdU and P-histone H3 in *AhCre⁺Apc^{fl/fl}p53^{-/-}* compared to *AhCre⁺Apc^{fl/fl}* (D4: Wt 87%; *AhCre⁺Apc^{fl/fl}* 23.73%; *AhCre⁺p53^{-/-}* 64.93%, *AhCre⁺Apc^{fl/fl}p53^{-/-}* 62.63%; D6: Wt 66.83%, *AhCre⁺Apc^{fl/fl}* 28.68%, *AhCre⁺p53^{-/-}* 55.09%, *AhCre⁺Apc^{fl/fl}p53^{-/-}* 59.49%). This shows that there is a net increase in the number of cells labelled during the S phase that are progressing through mitosis in the double mutant which supports our hypothesis of a G2 arrest after Apc loss and a bypass of this arrest in the P53 mutant.

Loss of Apc leads to an increase in anaphase bridges and aneuploidy, but this is not significantly enhanced by additional p53 deficiency

We next determined if additional loss of p53 affects the number of anaphase bridges observed after Apc loss. At D4, the anaphase bridge index was significantly elevated in *AhCre⁺Apc^{fl/fl}p53^{-/-}* compared to *AhCre⁺p53^{-/-}* (*AhCre⁺p53^{-/-}* 0.7% vs *AhCre⁺Apc^{fl/fl}p53^{-/-}* 14.86%: P=0.0022 MW) (Fig5D). A trend of higher levels of anaphase bridges was observed between *AhCre⁺Apc^{fl/fl}* and *AhCre⁺Apc^{fl/fl}p53^{-/-}* but the levels did not reach significance (*AhCre⁺Apc^{fl/fl}* 10.10%; *AhCre⁺Apc^{fl/fl}p53^{-/-}* 14.86% P=0.1358 MW). At D6, there is a similar trend again for both comparisons (P>0.05, MW). This data shows that the increase in anaphase bridges formation observed after Apc loss is not altered by p53 deficiency. However, it is worth noting that compared to Wt, Apc deficiency increased the number of anaphase bridge by 10 fold at D4 (4.56 times at D6), whereas in the double mutant this increase was 14.86 times at D4 (11.83 times at D6), but again this did not reach significance.

To test if combined deficiency of Apc and p53 resulted in a change in chromosome number, we performed short term primary liver culture. After β -naphthoflavone induction, Wt, *AhCre⁺Apc^{fl/fl}*, *AhCre⁺p53^{-/-}* and *AhCre⁺Apc^{fl/fl}p53^{-/-}* hepatocytes were analyzed for metaphase spreads (Fig6A). We noted that 60% of hepatocytes from *AhCre⁺Apc^{fl/fl}* have 60-80 chromosomes compared to 4% in Wt, 8.7% in *AhCre⁺P53^{-/-}* and 27% in *AhCre⁺Apc^{fl/fl}p53^{-/-}*. Similarly, 2.17% of hepatocytes from *AhCre⁺Apc^{fl/fl}* and 5.3% from *AhCre⁺Apc^{fl/fl}p53^{-/-}* have 100-120 chromosomes compared to none in Wt and *AhCre⁺p53^{-/-}* cells. Finally, we found that 6.8% of the hepatocytes from *AhCre⁺Apc^{fl/fl}* have 140-160 chromosomes compared to none in Wt, 1.6% in *AhCre⁺P53^{-/-}* and 0.4% in

$AhCre^+Apc^{fl/fl}p53^{-/-}$ These data indicates that loss of Apc leads to an increase in chromosome number compared to Wt and p53 deficient backgrounds. Given the above we observed a somewhat surprising decrease in the percentage of hepatocytes with 140-160 chromosome numbers in $AhCre^+Apc^{fl/fl}p53^{-/-}$ compared to $AhCre^+Apc^{fl/fl}$, which may reflect deletion of highly unstable cells as suggested by the high levels of Caspase3 positivity observed in the double mutants. Of additional note, comparison of levels of chromosomal aberration and the number of binucleated cells did not reveal a strong positive correlation.

Aneuploidy, an altered chromosome number, which is not a direct multiplication of the normal haploid number, is a common feature of human cancer [26]. Multiple defects occurring during mitosis such as mitotic checkpoint errors, can result in aneuploidy potentially through centrosome amplification [26-28]. To test if loss of Apc and combined deficiency of Apc and p53 affects centrosome numbers, we counted the number of centrosomes in hepatocytes for all genotypes at D4 and D6 after staining with a pericentrin antibody (Fig6B). We observed that compared to Wt, loss of Apc leads to a reduction of nuclei with one centrosome (as seen at D4 and D6, MW: $P<0.05$) which is balanced by a marked increase in nuclei with more than 2 centrosomes (D6: MW: $P<0.05$; D4: MW: $P>0.05$) (Fig6C-D). We next determined the effect of additional p53 deficiency upon centrosome amplification. We observed a significant reduction in the percentage of nuclei with one centrosome in $AhCre^+Apc^{fl/fl}p53^{-/-}$ compared to Wt and $AhCre^+p53^{-/-}$ (D4 and D6: MW: $P<0.05$) (Fig6C-D) and to a lesser extent compared to $AhCre^+Apc^{fl/fl}$ (D4 and D6, MW: $P>0.05$). This is coupled with an increase in the percentage of nuclei with more than 2 centrosomes in $AhCre^+Apc^{fl/fl}p53^{-/-}$ compared to Wt (D4 and D6, MW $P<0.05$), $AhCre^+P53^{-/-}$ (D4 MW: $P<0.05$, D6: MW $P>0.05$) but not compared to $AhCre^+Apc^{fl/fl}$ (D4 and D6, MW: $P>0.05$). In $AhCre^+p53^{-/-}$ hepatocytes, the levels of nuclei with 1 centrosomes were similar to Wt levels but the levels of nuclei with more than 2 centrosomes were increased compared to Wt levels (D4: MW: $P>0.05$, D6: MW $P<0.05$). Our data shows that loss of Apc leads to a significant increase in centrosome numbers however this phenotype is not affected by the addition of p53 deficiency. This could reflect the increase in apoptosis observed in the double mutant compared to $AhCre^+Apc^{fl/fl}$ where cells with more than 2 centrosomes are more susceptible to cell death.

Discussion

Activation of the Wnt pathway following loss of APC is one of the most important drivers of CRC and is also a key oncogenic event in HCC. For example, a recent extensive study in 125 HCC found that the Wnt/ β -catenin pathway was the most frequently altered pathway, with 32.8% of HCCs being mutated in CTNNB1, 15.2% in AXIN1, and 1.6% in APC genes [29]. However, there are other mechanisms by which Apc loss may impact upon tumorigenesis, as it is also implicated in the binding and stabilization of microtubules and chromosome segregation [6,7]. It is generally accepted that Apc loss occurs in the early stages of CRC, though its role in CIN is still debated. To study the role of the early loss of Apc in GI in the liver, we conditionally deleted Apc and found that Apc loss immediately drives increased proliferation which is accentuated by p53 deficiency. This is in contrast to

the situation in the small intestine, where p53 deficiency only weakly affects the phenotype of Apc loss [9].

To perform the analyses in the liver, we used two induction protocols, one harvested at D4 and one at D6. For the D4 time point we used our standard protocol (inducing male mice with 3 injections in 1 day), which results in near 100% recombination in both the intestine and liver. However, as our standard protocol compromises animal health beyond D4 due to the intestinal phenotype, the D6 time point was generated using a reduced induction protocol (a single injection of β -naphthoflavone) to minimize any adverse effects from recombination in the intestine. Surprisingly, the level of recombination in the hepatocytes, as assessed by nuclear β -catenin levels, was found to be similar at D4 and D6. All analyses were performed at both time points but some differences were observed. In the CTRLs, we observed differences in the levels of cleaved Caspase3 positive cells with a significant increase at D4 compared to D6. This may be due to the toxicity of the inducing agent β -naphthoflavone which has been shown to generate DNA damage and cell cycle check points [30]. At D6, we observed considerably less DSBs as identified by γ -H2AX staining compared to D4 (in *AhCre⁺p53^{-/-}*, *AhCre⁺Apc^{fl/fl}* and *AhCre⁺Apc^{fl/fl}p53^{-/-}* mutant). It is possible that the mouse at D6 was given more time to repair the DNA damage therefore showing less γ -H2AX staining compared to D4. P53 levels were similar at D4 and D6. However, in APC mutant samples, the level of Rad51 positive cells is lower at D4 compared to D6. This may again be due to the increase in time at D6, permitting a DNA damage response from the DNA repair pathways. A reduction in the number of aberrant bridges in *AhCre⁺Apc^{fl/fl}* and *AhCre⁺Apc^{fl/fl}p53^{-/-}* mutants was also observed at D6 compared to D4 which may also be due to the extended time available for either repair or elimination of abnormally dividing cells. Finally, we observed in *AhCre⁺Apc^{fl/fl}p53^{-/-}* mutant but not in the *AhCre⁺Apc^{fl/fl}* mutant an increase at D6 of cells with nuclei with more than 2 centrosomes compared to D4. This could be due to the additional loss of P53 which in the D6 time point is permissive for the Apc mutant cells to develop genomic instability. Some trends and differences were also observed with the FACS analysis. The trend for an increase in the 4N population between D4 and D6 did not reach significance (P=0.2593), however a significant difference was observed in the proportion of nuclei with greater than 4N DNA content (18.4% at D4 vs 7.6% at D6). Again, this may reflect an increase in the elapsed time from induction.

The increase in proliferation following Apc loss is associated with hepatomegaly. This has been previously reported [19] and correlates with β -catenin activation and ultimately HCC [13]. However, we do not see a further increase in liver size in *AhCre⁺Apc^{fl/fl}p53^{-/-}*, despite observing elevated proliferation. Hence, in our model there is dissociation between hepatomegaly and proliferation. This dissociation may reflect the increased levels of apoptosis we observe in *AhCre⁺Apc^{fl/fl}p53^{-/-}*, with the increased loss of hepatocytes compensating for the increased proliferation.

One likely reason for the increased rate of apoptosis is an increase in DNA damage, as evidenced by the accumulation of DSBs (γ H2AX) and presence of DNA repair (Rad51). DSBs are a major threat to genome integrity and DSB repair pathways have evolved to preserve cell survival and DNA integrity [31]. The increase in Rad51 and γ H2AX positive cells indicates elevated DNA damage following loss of Apc, the repair of which is normally

mediated by p53. The consequence of this is elevated cell death in the double mutant, which is clearly occurring in a p53-dependent manner.

The key question is how does Apc loss lead to elevated DNA Damage? Recently it has been shown that mitotic spindle defects can generate DSBs by centromere shearing [32]. As Apc loss leads to mitotic spindle defects [33], it is therefore possible that the DSBs observed are a direct consequence of spindle defects.

Previous studies have suggested a role for Apc within the cell cycle. Our data shows an accumulation of cells with 4N DNA content which is consistent with a G2 arrest. APC has been shown to localize to kinetochores, centrosomes and microtubules [7]. Indeed APC may regulate kinetochore microtubule attachment at centrosomes and this could influence mitosis. We show that the effects observed on 2N and 4N DNA content after Apc loss are dependent upon the presence of functional p53. p53 has been shown previously to play a role in both the G1/S and G2/M arrests which are mechanisms employed by the cells to prevent GI [34,35]. To further explore the role of p53 we performed double labelling with antibodies to BrdU and P-histone H3 to analyse progression from G2 to M phase. At both D4 and D6 we observed a decrease in the percentage of doubly labelled cells in the APC mutants compared to Wt, thereby suggesting G2/M arrest. However, additional loss of p53 led to a partial rescue of this phenotype to almost Wt levels. These data indicate that additional loss of p53 enables some of the cells to progress through the G2-M phase. We therefore suggest that Apc loss leads to a G2/M arrest and that p53 plays a role in maintaining this arrest.

Our FACS data indicate that in a p53 deficient background, Apc loss leads to an increase in DNA content greater than 4N and consistent with aneuploidy. This increase is concomitant with an increase in anaphase bridges. We observe that anaphases bridges occur even in the early stages of Apc loss. Anaphase bridges are susceptible to breakages [36, 37] which results in gross chromosomal rearrangements, translocations, or deletion. Similarly, aberrant mitotic division has been shown to result in aneuploidy [38]. Anaphase bridges in ES cells carrying *Apc^{Min}* were correlated with an increase or decrease in chromosome numbers suggesting aneuploidy [4]. Our data shows a change in the chromosome number correlated with an increase in centrosome number after loss of Apc. Increase in centrosome number has been linked to failure to complete cytokinesis and skipping mitosis. It is well established that centrosome amplification contributes to aneuploidy which is linked to chromosome segregation errors during mitosis [28]. All of this data is in accordance with an early role for Apc in maintaining euploidy. However, our data also show that p53 deficiency does not enhance the effects of Apc loss on anaphase bridge formation and centrosome amplification. This is in contrast with the data observed for γ H2AX, Rad51, cell proliferation, cell death and DNA content where the addition of p53 deficiency significantly increases the Apc loss phenotype which supports the role of p53 in protecting the genome against mitotic defects and aneuploidy. It is therefore possible that the marginal effect of p53 deficiency after Apc loss on anaphase bridge formation, chromosome number and centrosome amplification is due to the increase cell death observed in the double mutant. For example, the cells in the double mutant could have undergone mitotic catastrophe leading to cell death with the net result of a marginal increase in anaphase bridge formation, chromosome number and

centrosome amplification. This mechanism, which has been previously described [39], would therefore limit the extent of genomic instability.

As discussed above, Apc plays a critical role in regulating the levels of activated β -catenin. A role for β -catenin in CIN has also been described [40], and one could argue that the aneuploidy we observe is directly due to activation of β -catenin. Conversely, there are data which show that in *Apc^{Min}* mice aneuploidy is observed in intestinal cells with a normal level of activated β -catenin [41]. Clearly, further studies are needed to define the extent to which activated β -catenin may drive aneuploidy in the absence of Apc.

Previously it was shown that Apc loss in the small intestine rapidly leads to tetraploidy but that p53 has very little role in this process although the loss of p53 did alter the transcriptome following Apc loss [5]. In the longer term, p53 deficiency again only marginally altered intestinal adenoma predisposition in the *Apc^{Min}* mouse [42]. By contrast, Apc and p53 mutations have been shown to synergise in driving renal tumourigenesis [10], although limited short term data has been reported. The data we show here suggest that p53 status is more important in controlling Wnt driven genomic instability in hepatocytes as compared to enterocytes. Given the lack of immediate genomic instability data from the kidney and also the lack of long term tumourigenesis data from the liver, this makes tissue specific comparisons difficult, and indeed highlights the need for additional studies.

In summary, our data shows that Apc deficiency leads to perturbation of the cell cycle, elevated DNA damage, the accumulation of p53 and apoptosis. We show that anaphase bridges occur even in the early stages of Apc loss, suggesting the development of aneuploidy. Our data also show an increase in chromosome and centrosome numbers after loss of Apc confirming a role for Apc in maintaining euploidy. In the additional absence of p53, many of these effects are accentuated suggesting that p53 has a role in protecting the genome against mitotic defects generated by the loss of Apc however this does not result in a clear increase in anaphase bridges and centrosome numbers. Our data suggest that combined Apc and p53 deficiency does enhance the signal of DNA damage but this does not translate into immediate enhanced genomic instability as the DNA damage signal may be at least partially compensated for by elevated cell death through mitotic catastrophe.

Material and Methods

Experimental animals

All experiments were performed under the U.K. Home Office guidelines. Outbred mice segregating for the C57BLJ and S129 genomes (6-12 weeks) were used. Mice were obtained and genotyped as follows: *Apc^{580S}* (*Apc^{fl}*) [20], *AhCre* [21], *p53null* (*p53^{-/-}*) [22]. Mice *AhCre⁺Apc^{fl/fl}* (APC), *AhCre⁺p53^{-/-}* (P53), *AhCre⁺Apc^{fl/fl}p53^{-/-}* (APCP53) and Wt (*AhCre⁻Apc^{fl/+}*, *AhCre⁺Apc^{fl/+}*, *AhCre⁺Apc^{+/+}*) were generated. To investigate the phenotype of conditional deletion of Apc, mice bearing a lox-flanked *Apc* allele were crossed onto inducible cre transgenic, which uses the *Cyp1A* promoter to deliver inducible cre expression in the liver and the intestine. Recombination was induced in mice by three intraperitoneal (i.p.) injections (at 4 hour intervals) in 1 day (Day0) of 80mg/kg β -naphthoflavone and sacrificed and dissected 4 days later at Day4 (D4) or induced with one

i.p injection of 80mg/kg (Day0) and sacrificed and dissected 6 days later at Day6 (D6). For proliferation analysis, mice were injected either 2hrs or 24hrs before culling with 0.25 ml of BrdU (Amersham).

Histology and Immunohistochemistry

Liver tissue was fixed in ice-cold 10% formalin and paraffin embedded tissue sections (5 μ m) were used for immunohistochemistry (IHC). Ki67, Caspase3, BrdU, P21, p53, γ H2AX immunohistochemistry (IHC) were performed as previously described [9, 19]. For Rad51 IHC (mouse monoclonal, 1:25 Labvision), antigen retrieval was performed in 1 \times citrate buffer in microwave pressure cooker. We used 2 $^{\circ}$ antibody from Vectastain mouse-ABC kit (Vector-labs). Positive cells from 5-10 field of view were counted (around 1000cells) per mouse. For very low frequency events such as Caspase3, BrdU, we counted 10 fields at 200x magnification, the number of cells counted per mouse is around 1000. For each count, at least 3 animals per genotype were counted. When stated 200 nuclei were counted it is 200nuclei/animal/genotype.

Immunofluorescence for double labelling of BrdU and phospho-histone H3

Liver tissue was fixed in ice-cold 10% formalin and paraffin embedded tissue sections (5 μ m) were used for IHC. Antigen retrieval was performed in 1 \times citrate buffer in microwave pressure cooker. We used 1/200 dilution of BrdU plus Phospho-histone H3 antibodies (phospho-histone H3:Cell signalling #9701; BrdU BD). Phospho-histone H3 (P-histone H3) was detected using a biotinylated goat Anti-Rabbit antibody (Dako) and the AB reagents from Vectastain (Vector labs). The fluorescent signal was provided using the Fluorescein Tyramide Signal Amplification (TSA) Systems (Perkin elmer). BrdU antibody was detected using a goat anti mouse 1/200 Alexa 568 antibody (Molecular Probes life technologies). Cells were counterstained with Dapi (500ng/ml) and slides were mounted with mowiol. Pictures were taken using a Leica DMI6000 time lapse microscope.

Nuclear area

The area (μ m²) of nuclei was assessed using Hematoxylin-Eosin (H and E) stained section after image capture using Analysis software (Soft Imaging Systems). At least 200 nuclei per mouse from N=3 or more mice of each genotype were measured and the moving average test was used to analyze the data.

DNA content using Flow cytometry

Fresh livers were minced with a scalpel. Cells were suspended in 1ml of 0.1M citric acid, 0.5% vol/vol Tween20 solution, shaken for 20min at 20°C, passed through a 50-100- μ m sieve and fixed with 70% ethanol. DRAQ5 (Biostatus-limited) was added to a concentration of 20 μ M before the detection of DNA content using FACS-caliber (Becton-Dickinson). Percentage of cells with 2N DNA content, 4N, DNA content between 2N and 4N (S phase) or greater than 4N (4N<) was determined for each mice, from N=3 or more mice of each genotype. 10 000 events were counted in total for each mouse. The data generated are given as a percentage for each DNA content 2N, S, 4N, and greater than 4N. The percentage for

each mouse of the same genotype was averaged for each DNA content and error bars showing standard errors were calculated and used to show the variation.

Liver culture and chromosome spread

Mouse Primary hepatocytes were isolated by liver perfusion medium using a 2-step retrograde procedure. Hepatocytes were purified using percoll-gradient and plated on a fibronectin coated plate as previously described [23]. Chromosome spreads were generated after 2 days of culture. 2hrs before harvest, hepatocytes in culture were supplemented with ethidium bromide (1.5µg/ml). Colcemid (Karyomax) was added (0.1µg/ml) 40min later and left for 80min at 37°C. Cells were then collected and resuspended in 75mM KCL for 5min and fixed with ice-cold Methanol-acetic-acid solution (3/1Volume). Cells were analysed for chromosomes numbers (at least 20 chromosome spreads were counted).

Centrosome staining

Liver cryosections (5µm) were fixed with 4% paraformaldehyde and blocked for 1 hour with mouse IgG blocking reagent (vector labs). After blocking with Donkey serum (5% in PBS-0.3% Tween), sections were incubated with 1/500 anti-pericentrin antibody (Abcam) overnight. Secondary 1/500 Anti-rabbit Cy3 (Jackson immunoresearch, stratech) and 1/500 Alexafluor 488 –phalloidin (invitrogen) was then applied on the sections for 1-2hours. Sections were mounted with vectashield plus DAPI medium. Sections were viewed and analysed using a Leica TCS SP2 spectral confocal microscope and Leica confocal software (Leica, Heidelberg, Germany). Centrosomes numbers were counted in at least 150 nuclei of hepatocytes from each mouse for each genotype (N=3-5) at D4 and D6.

Statistics

Histograms comparison was performed using Mann-Whitney U test (MiniTab). Cumulative frequency and % nuclear size comparison was performed using the Kolmogorov-Smirnov test. For the anaphase bridges data, in the control cohort D4, there was no variation with all values being zero. Mann Whitney test completion was impossible because all values in one column were identical. We therefore used a bootstrapping method in order to perform a more powerful statistical test on the data and determine the 95% confidence intervals. The mean of the *AhCre⁺Apc^{fl/fl}* group D4 was bootstrapped, therefore, groups were assessed as significantly different if *AhCre⁺Apc^{fl/fl}* 95% confidence intervals did not overlap this zero value.

Supplementary Material

Refer to Web version on PubMed Central for supplementary material.

ACKNOWLEDGMENTS

We thank Mark Bishop (genotyping) and Derek Scarborough (histology).

Financial support: Cancer research UK RCBMA7613

Abbreviations

DSBs	Double strand breaks
MW	Mann-Whitney
CIN	chromosomal instability
GI	genomic instability
D4	Day4
D6	Day6
CRC	colorectal cancer
HCC	Hepatocellular carcinoma
Apc	Adenomatous polyposis coli

References

- [1]. Fearon ER. Molecular genetics of colorectal cancer. *Annu Rev Pathol.* 2011; 6:479–507. [PubMed: 21090969]
- [2]. Clevers H. Wnt/ β -Catenin Signaling in Development and Disease. *Cell.* 2006; 127:469–480. [PubMed: 17081971]
- [3]. Fodde R, Kuipers J, Rosenberg C, Smits R, Kielman M, Gaspar C, et al. Mutations in the APC tumor suppressor gene cause chromosomal instability. *Nat Cell Biol.* 2001; 3:433–438. [PubMed: 11283620]
- [4]. Kaplan KB, Burds AA, Swedlow JR, Bekir SS, Sorger PK, Näthke IS. A role for the Adenomatous Polyposis Coli protein in chromosome segregation. *Nat Cell Biol.* 2001; 3:429–432. [PubMed: 11283619]
- [5]. Dikovskaya D, Schiffmann D, Newton IP, Oakley A, Kroboth K, Sansom O, et al. Loss of APC induces polyploidy as a result of a combination of defects in mitosis and apoptosis. *The Journal of Cell Biology.* 2007; 176:183–195. [PubMed: 17227893]
- [6]. Hanson CA, Miller JR. Non-traditional roles for the Adenomatous Polyposis Coli (APC) tumor suppressor protein. *Gene.* 2005; 361:1–12. [PubMed: 16185824]
- [7]. Rusan NM, Peifer M. Original CIN: reviewing roles for APC in chromosome instability. *J Cell Biol.* 2008; 181:719–726. [PubMed: 18519734]
- [8]. Shih IM, Zhou W, Goodman SN, Lengauer C, Kinzler KW, Vogelstein B. Evidence that genetic instability occurs at an early stage of colorectal tumorigenesis. *Cancer Res.* 2001; 61:818–822. [PubMed: 11221861]
- [9]. Reed KR, Meniel VS, Marsh V, Cole A, Sansom OJ, Clarke AR. A limited role for p53 in modulating the immediate phenotype of Apc loss in the intestine. *BMC Cancer.* 2008; 8:162. [PubMed: 18533991]
- [10]. Sansom OJ, Griffiths DF, Reed KR, Winton DJ, Clarke AR. Apc deficiency predisposes to renal carcinoma in the mouse. *Oncogene.* Dec 8; 2005 24(55):8205–10. [PubMed: 16116480]
- [11]. Aoki K, Aoki M, Sugai M, Harada N, Miyoshi H, Tsukamoto T, et al. Chromosomal instability by β -catenin/TCF transcription in APC or β -catenin mutant cells. *Oncogene.* 2007; 26:3511–3520. [PubMed: 17160019]
- [12]. Torre C, Perret C, Colnot S. Transcription dynamics in a physiological process: beta-catenin signaling directs liver metabolic zonation. *Int J Biochem Cell Biol.* 2011; 43:271–278. [PubMed: 19914393]
- [13]. Gougelet A, Colnot S. A Complex Interplay between Wnt/ β -Catenin Signalling and the Cell Cycle in the Adult Liver. *Int J Hepatol.* 2012; 2012:816125. [PubMed: 22973520]

- [14]. Laurent-Puig P, Zucman-Rossi J. Genetics of hepatocellular tumors. *Oncogene*. 2006; 25(27): 3778–86. [PubMed: 16799619]
- [15]. Feng GJ, Cotta W, Wei XQ, Poetz O, Evans R, Jardé T, et al. Conditional disruption of Axin1 leads to development of liver tumors in mice. *Gastroenterology*. Dec; 2012 143(6):1650–9. [PubMed: 22960659]
- [16]. Jain S, Chang TT, Hamilton JP, Lin SY, Lin YJ, Evans AA, et al. Methylation of the CpG sites only on the sense strand of the APC gene is specific for hepatocellular carcinoma. *PLoS One*. 2011; 6(11):e26799. [PubMed: 22073196]
- [17]. Hussain SP, Schwank J, Staib F, Wang XW, Harris CC. TP53 mutations and hepatocellular carcinoma: insights into the etiology and pathogenesis of liver cancer. *Oncogene*. 2007; 26:2166–2176. [PubMed: 17401425]
- [18]. Pineau P, Marchio A, Battiston C, Cordina E, Russo A, Terris B, et al. Chromosome instability in human hepatocellular carcinoma depends on p53 status and aflatoxin exposure. *Mutation Research*. 2008; 653:6–13. [PubMed: 18467159]
- [19]. Reed KR, Athineos D, Meniel VS, Wilkins JA, Ridgway RA, Burke ZD, et al. B-catenin deficiency, but not Myc deletion, suppresses the immediate phenotypes of APC loss in the liver. *Proc Natl Acad Sci USA*. 2008; 105(48):18919–23. [PubMed: 19033191]
- [20]. Shibata H, Toyama K, Shioya H, Ito M, Hirota M, Hasegawa S, et al. Rapid colorectal adenoma formation initiated by conditional targeting of the Apc gene. *Science*. 1997; 278:120–123. [PubMed: 9311916]
- [21]. Ireland H, Kemp R, Houghton C, Howard L, Clarke AR, Sansom OJ. Inducible Cre-mediated control of gene expression in the murine gastrointestinal tract: effect of loss of beta-catenin. *Gastroenterology*. 2004; 126(5):1236–1246. [PubMed: 15131783]
- [22]. Clarke AR, Purdie CA, Harrison DJ, Morris RG, Bird CC, Hooper ML, et al. Thymocyte apoptosis induced by p53-dependent and independent pathways. *Nature*. 1993; 362:849–851. [PubMed: 8479523]
- [23]. Prost S, Sheahan S, Rannie D, Harrison DJ. Adenovirus-mediated Cre deletion of floxed sequences in primary mouse cells is an efficient alternative for studies of gene deletion. *Nucleic Acids Res*. 2001; 29(16):E80. [PubMed: 11504888]
- [24]. Sansom OJ, Reed KR, Hayes AJ, Ireland H, Brinkmann H, et al. Loss of Apc in vivo immediately perturbs Wnt signaling, differentiation, and migration. *Genes Dev*. 2004; 18:1385–1390. [PubMed: 15198980]
- [25]. Hans F, Dimitrov S. Histone H3 phosphorylation and cell division. *Oncogene*. May 28; 2001 20(24):3021–7. Review. [PubMed: 11420717]
- [26]. Weaver BA, Cleveland DW. Does aneuploidy cause cancer? *Curr Opin Cell Biol*. Dec; 2006 18(6):658–67. Epub 2006 Oct 12. Review. Erratum in: *Curr Opin Cell Biol*. 2007 Apr;19(2):246. [PubMed: 17046232]
- [27]. Godinho SA, Pellman D. Causes and consequences of centrosome abnormalities in cancer. *Philos Trans R Soc Lond B Biol Sci*. Sep 5.2014 369(1650) pii: 20130467. Review.
- [28]. Vitre BD, Cleveland DW. Centrosomes, chromosome instability (CIN) and aneuploidy. *Curr Opin Cell Biol*. Dec; 2012 24(6):809–15. [PubMed: 23127609]
- [29]. Guichard C, Amaddeo G, Imbeaud S, Ladeiro Y, Pelletier L, Maad IB, et al. Integrated analysis of somatic mutations and focal copy-number changes identifies key genes and pathways in hepatocellular carcinoma. *Nat Genet*. May 6; 2012 44(6):694–8. [PubMed: 22561517]
- [30]. Vaziri C, Faller DV. A benzo[a]pyrene-induced cell cycle checkpoint resulting in p53-independent G1 arrest in 3T3 fibroblasts. *J Biol Chem*. Jan 31; 1997 272(5):2762–9. [PubMed: 9006915]
- [31]. Bree RT, Neary C, Samali A, Lowndes NF. The switch from survival responses to apoptosis after chromosomal breaks. *DNA Repair*. 2004; 3:989–995. [PubMed: 15279785]
- [32]. Guerrero AA, Gamero MC, Trachana V, Fütterer A, Pacios-Bras C, Díaz-Concha, et al. Centromere-localized breaks indicate the generation of DNA damage by the mitotic spindle. *Proc Natl Acad Sci USA*. 2010; 107(9):4159–64. [PubMed: 20142474]

- [33]. Dikovskaya D, Newton IP, Nathke IS. The adenomatous polyposis coli protein is required for the formation of robust spindles formed in CSF Xenopus extracts. *Mol. Biol. Cell.* 2004; 15:2978–2991. [PubMed: 15075372]
- [34]. Bunz F, Dutriaux A, Lengauer C, Waldman T, Zhou S, Brown JP, et al. Requirement for p53 and p21 to sustain G2 arrest after DNA damage. *Science.* 1998; 282:1497–501. [PubMed: 9822382]
- [35]. Cross SM, Sanchez CA, Morgan CA, Schimke MK, Ramel S, Idzerda RL, et al. A p53-dependent mouse spindle checkpoint. *Science.* 1995; 267:1353–1356. [PubMed: 7871434]
- [36]. Gisselsson D, Jonson T, Petersen A, Strombeck B, Dal Cin P, Hoglund M, et al. Telomere dysfunction triggers extensive DNA fragmentation and evolution of complex chromosome abnormalities in human malignant tumors. *Proc Natl Acad Sci USA.* 2001; 98:12683–12688. [PubMed: 11675499]
- [37]. Hoffelder DR, Luo L, Burke NA, Watkins SC, Gollin SM, Saunders WS. Resolution of anaphase bridges in cancer cells. *Chromosoma.* 2004; 112:389–397. [PubMed: 15156327]
- [38]. Kops GJ, Weaver BA, Cleveland DW. On the road to cancer: aneuploidy and the mitotic checkpoint. *Nature reviews. Cancer.* 2005; 5:773–785. [PubMed: 16195750]
- [39]. Castedo M, Perfettini JL, Roumier T, Andreau K, Medema R, Kroemer G. Cell death by mitotic catastrophe: a molecular definition. *Oncogene.* 2004; 23:2825–2837. [PubMed: 15077146]
- [40]. Hadjihannas MV, Behrens J. CIN By WNT Growth Pathways, Mitotic Control and Chromosomal Instability in Cancer. *Cell Cycle.* 2006; 5(18):2077–2081. [PubMed: 16969101]
- [41]. Caldwell CM, Green RA, Kaplan KB. APC mutations lead to cytokinetic failures in vitro and tetraploid genotypes in Min mice. *J Cell Biol.* 2007; 178:1109–20. [PubMed: 17893240]
- [42]. Clarke AR, Cummings MC, Harrison DJ. Interaction between murine germline mutations in p53 and APC predisposes to pancreatic neoplasia but not to increased intestinal malignancy. *Oncogene.* Nov 2; 1995 11(9):1913–20. [PubMed: 7478622]

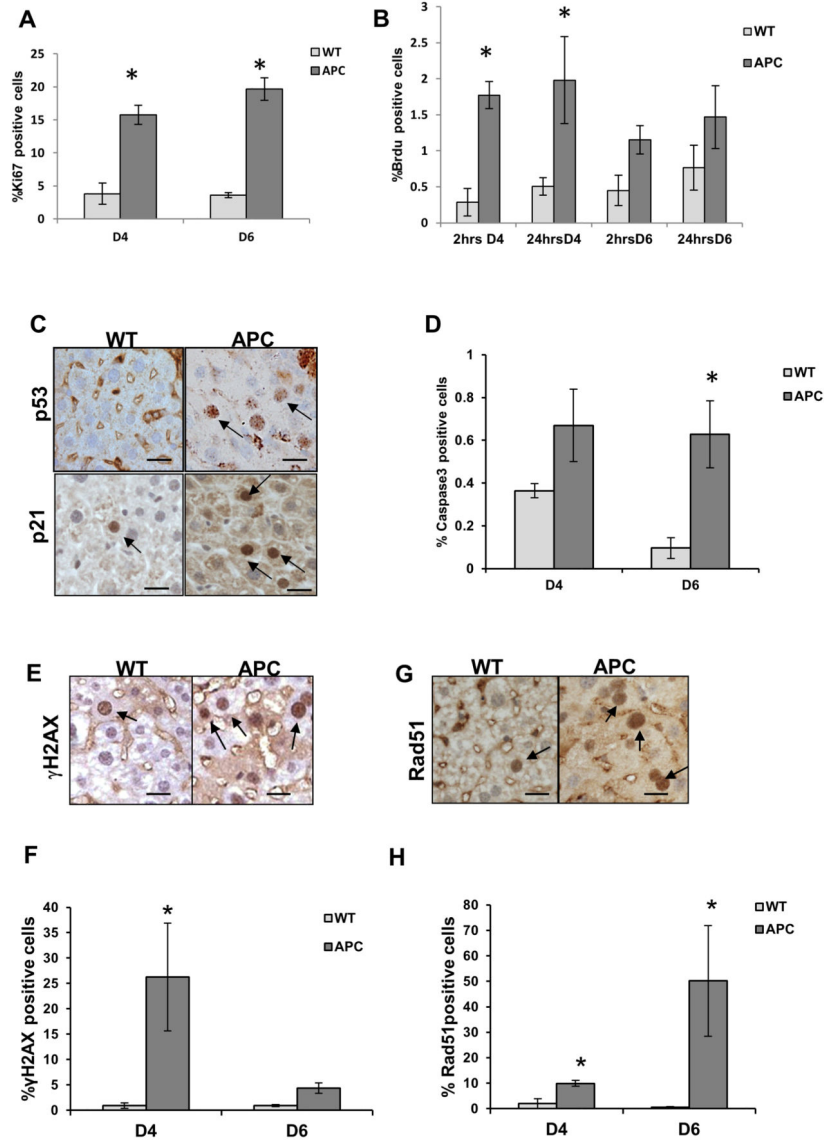


Fig.1. Loss of Apc in the liver leads to DNA damages, DNA repair and proliferation
(A) Increased %Ki67 labelling at D4 and D6 in APC versus Wt. **(B)** Increased %BrdU labelling after 2hrs BrdU in APC (D4 and D6) versus Wt. Similar %BrdU labelling from 2hrs to 24hrs in Wt or APC. **(C)** p53 and p21 increased levels in APC versus Wt. **(D)** Increased %Caspase3 at D6 or D4 in APC versus Wt. **(E,F)** γ H2AX staining and scoring **(G,H)** Rad51 staining and scoring in APC versus Wt at D4 and D6. Increased % γ H2AX or %Rad51 labelling in APC versus Wt. Bars indicate standard-error. * indicates $P < 0.05$ MW (N=3 mice). Arrows indicate Positive cells (Scale=10 μ m). Wt, *AhCre⁺Apc^{fl/fl}* (APC)

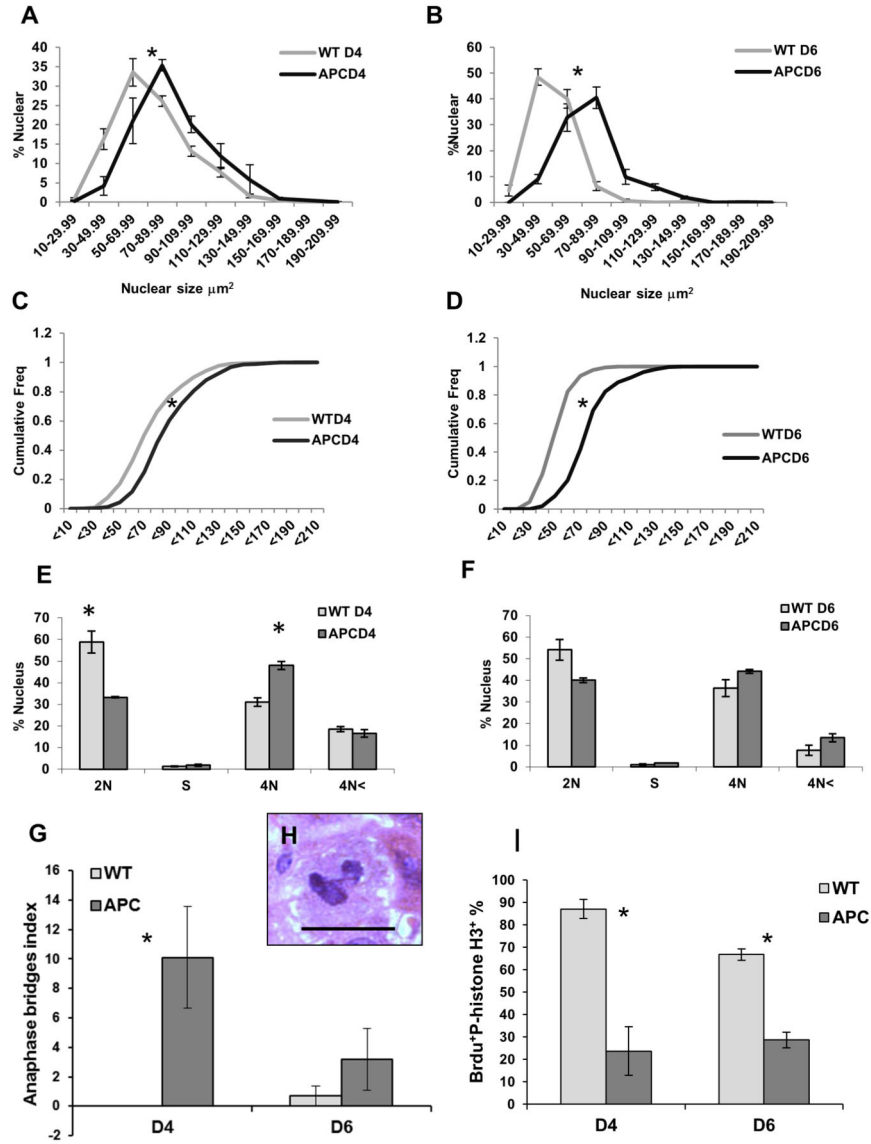


Fig.2. *Apc* deficiency leads to increased apoptosis, nuclear area, 4N DNA content, cell cycle perturbation and anaphase bridges and decreased of BrdU⁺P-histone H3⁺ cells
 Increase in nuclear area (μm²) (%=A+B; Cumulative-Frequency=C+D) at D4 (A+C) and D6 (B+D) in APC versus Wt (P=0.01 Kolmogorov-Sminov). (E-F) DNA content by Flow cytometry of hepatocytes at D4 (E) or D6 (F). Decrease in % of cells with 2N DNA content and increase in 4N DNA content in APC versus Wt. (G) Increased anaphase bridges index in APC versus Wt. (H) Anaphase bridge in hepatocyte. (I) Dual immunostaining with P-histone H3 and BrdU 24hrs after injection of BrdU was compared to Brdu positive cells. Decrease in % of cells with double labelling in APC versus Wt. Bars indicate standard-error. * indicates P<0.05 MW. (N 3 mice) (Scale=50μm). Wt, *AhCre⁺Apc^{fl/fl}* (APC)

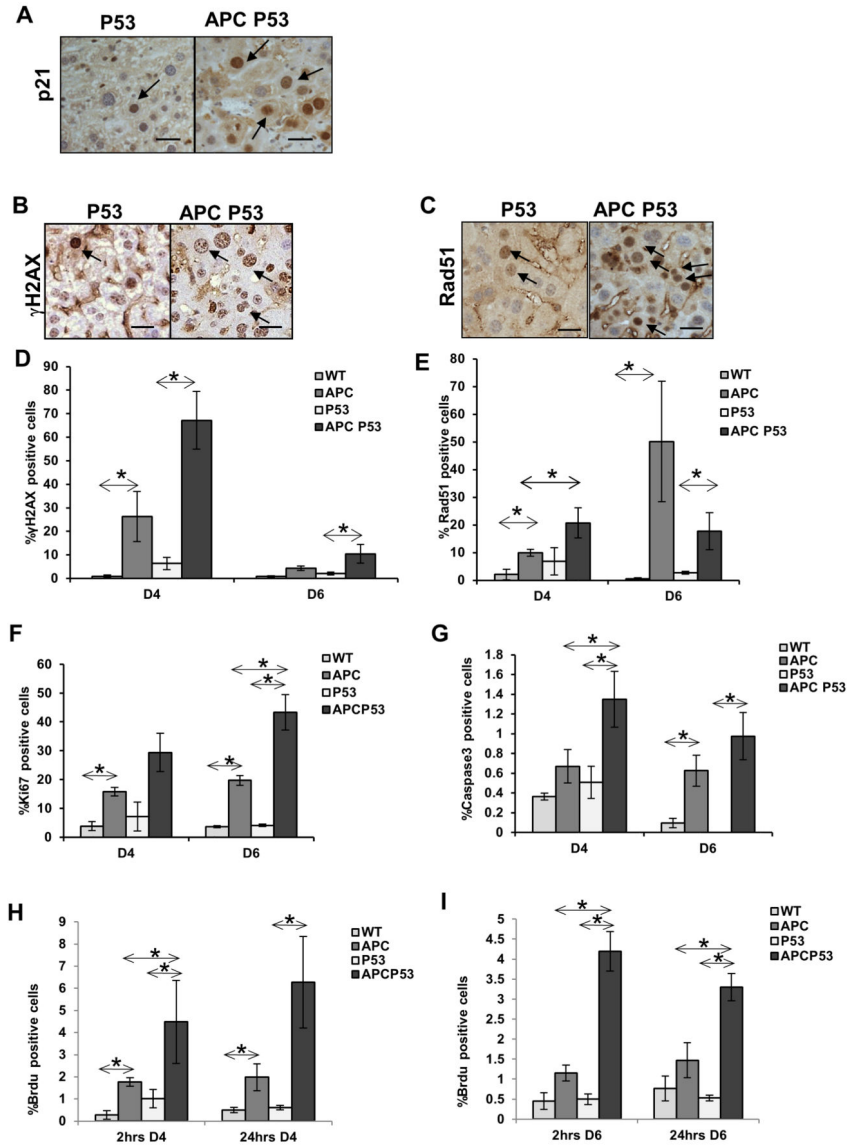


Fig.3. P53 deficiency enhances DNA damage, DNA repair, proliferation and apoptosis induced by Apc loss

(A) Increased p21 levels in APCP53 versus P53. (B) γ H2AX staining. (C) Rad51 staining. (D) Scoring of γ H2AX positive cells. (E) Scoring of Rad51 positive cells. Increased % γ H2AX or %Rad51 labelling in APCP53. (F) Increased %Ki67 labelling at D4 and D6 in APCP53 (G) Increased %Caspase3 at D6 or D4 in APCP53. (H-I) Increased %BrdU labelling after 2hrs in APCP53 at D4 (H) and D6 (I). No increase is seen in %BrdU labelling from 2hrs to 24hrs in APCP53.; Bars indicate standard-error. * indicates $P < 0.05$ MW, (N=3 mice). Arrows indicate positive cells, (Scale=10 μ m). Wt, $AhCre^+Apc^{fl/fl}$ (APC), $AhCre^+P53^{-/-}$ (P53), $AhCre^+Apc^{fl/fl}p53^{-/-}$ (APCP53)

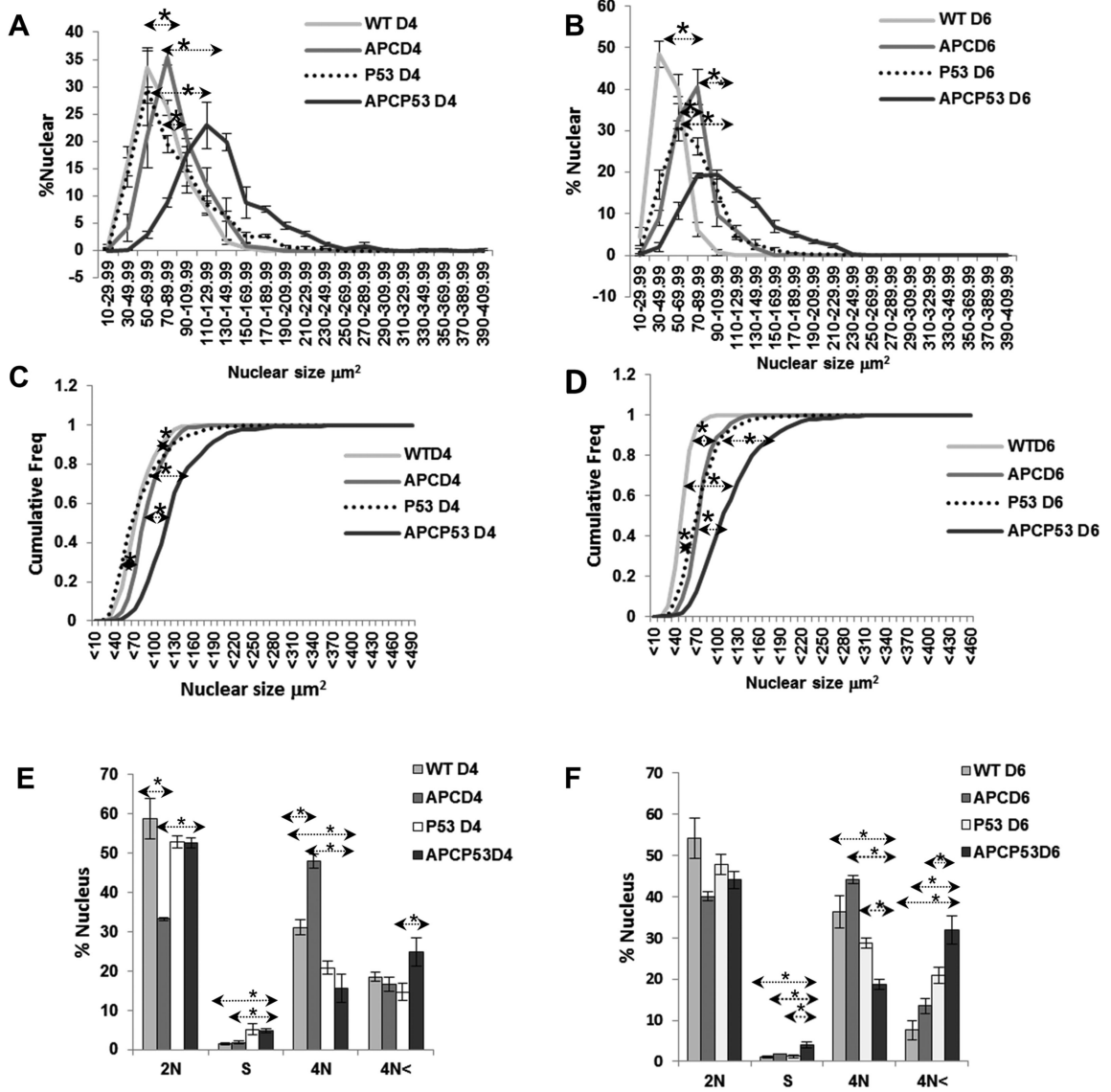


Fig.4. P53 deficiency enhances increased nuclear area, 4N DNA content, cell cycle perturbation induced after *Apc* loss

Increase in nuclei area (μm^2) (%=A+B; Cumulative-frequency=C+D) at D4 (A+C) and D6 (B+D) in APCP53 versus P53 and APC (P=0.01 Kolmogorov-Smirnov). (E-F) DNA content by Flow cytometry of hepatocytes at D4 (E) or D6 (F) in APC, P53 and APCP53. Increase in cells with DNA content greater than 4N in APCP53. Bars indicate standard-error. * indicates P<0.05 MW, (N 3 mice). Wt, *AhCre⁺Apc^{fl/fl}* (APC), *AhCre⁺P53^{-/-}* (P53), *AhCre⁺Apc^{fl/fl}p53^{-/-}* (APCP53)

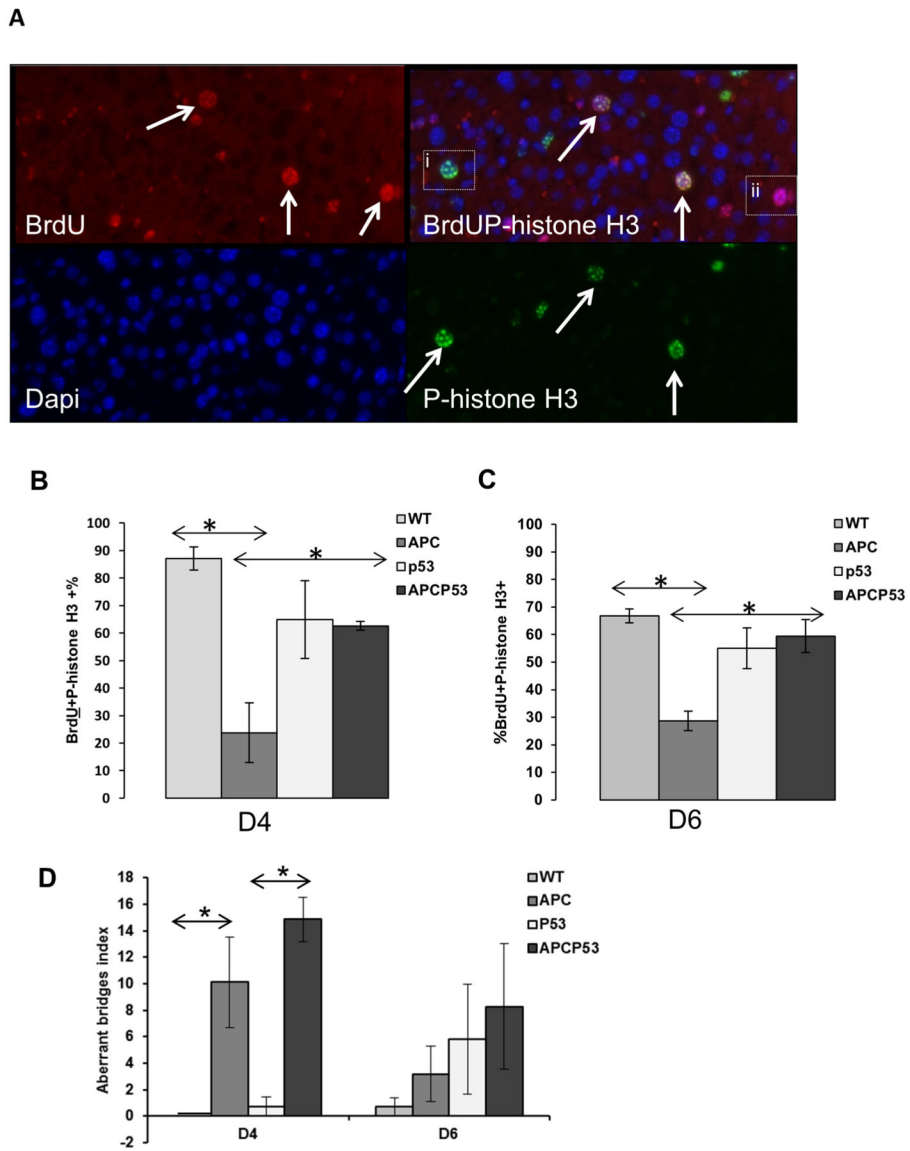


Fig.5. P53 deficiency does not enhance anaphases bridges after Apc loss but leads to partial rescue of BrdU⁺P-histoneH3⁺ cells number
(A) Dual immunostaining with P-histone H3 and BrdU 24hrs (BrdU⁺P-histone H3⁺) was compared to BrdU positive cells (BrdU⁺). **(i)** shows a P-histone H3⁺ positive cell but negative for BrdU labelling; **(ii)** shows a BrdU⁺ cell but negative for P-histone H3 labelling, White arrows indicate positive cells. **(B)** Increased number of BrdU⁺P-histone H3⁺ in APCP53 compared to APC at D4. **(C)** Increased number of BrdU⁺P-histone H3⁺ in APCP53 compared to APC at D6. **(D)** Increased anaphase bridges index in APCP53. Bars indicate standard-error. * indicates P<0.05 MW, (N 3 mice). Wt, *AhCre⁺Apc^{fl/fl}* (APC), *AhCre⁺P53^{-/-}* (P53), *AhCre⁺Apc^{fl/fl}p53^{-/-}* (APCP53)

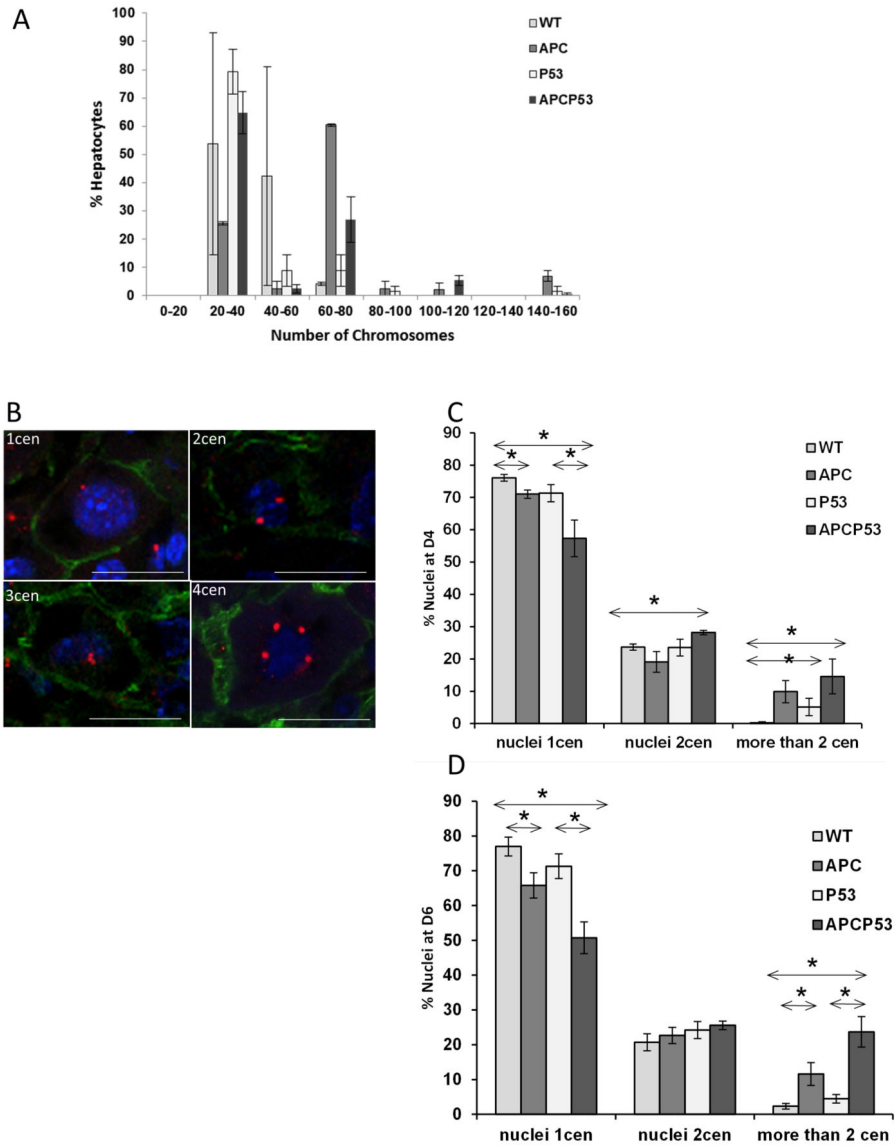


Fig.6. Apc loss leads to aneuploidy and increase in centrosomes number which is not significantly enhanced by additional P53 deficiency

(A) Chromosome numbers per hepatocytes in Wt, APC, APCP53 versus P53 with abnormal numbers in APC and APCP53 (N = 2). Bars indicate standard-error. * indicates P<0.05. (B) centrosomes staining (red) representative pictures. cen = centrosome. (Scale=50µm) (C) % nuclei with 1 cen (cen=centrosome), or 2 cen or more than 1 cen. Increase in nuclei with more than 2 centrosomes in APC versus Wt at D4 and D6. This Increase is not significantly altered in APCP53 compared to APC at D6 and D4. Bars indicate standard-error. * indicates P<0.05 MW, (N=3-5 mice). Wt, *AhCre⁺Apc^{fl/fl}* (APC), *AhCre⁺P53^{-/-}* (P53), *AhCre⁺Apc^{fl/fl}p53^{-/-}* (APCP53)